JOURNAL OF THEORETICAL
AND APPLIED MECHANICS
2, **40**, 2002

APPLICATION OF THE PROJECTIVE INPUT RESIDUAL METHOD TO DIAGNOSIS OF FAILURE MECHANICAL SYSTEMS

Bartosz Powałka
Krzysztof Marchelek

Institute of Manufacturing Engineering, Technical University of Szczecin
e-mail: bartps@safona.tuniv.szczecin.pl

The paper is concerned with the method of failure detection on the basis of incomplete measurements, which means that the number of measured signals is lower than the number of degrees of freedom of mechanical systems. The method does not require the reduction of the number of degrees of freedom of the mathematical model and therefore the identified parameters can be physically interpreted. The proposed indicator used to detect the damaged element is based on the comparison of partial derivatives of the input residuals of the damaged and undamaged models. The method will be illustrated with an example of FWD-32J milling machine.

Key words: milling machine, damage diagnosis

1. Introduction

Machines during their exploitation are exposed to wear of the co-operating elements. The wear, in the case of responsible constructions such as bridges etc. May lead tragic consequences if not detected sufficiently early. Therefore, the development of methods focused on the detection of damages (or changes) in mechanical systems is justified.

A number of dynamics-based methods have been developed in the past for detection of changes due to damage (Doebling et al., 1996). To provide efficient inspections of complex mechanical systems model-dependent methods are used. These methods in combination with real measurements, are generally more accurate in locating damage than measurement alone (Natke et al., 1993). The methods which use only dynamic responses can detect the existence of damage but do not allow one to indicate its location. At the forefront of the hybrid methods (Li et al., 1995), i.e. combinations of model and measurement based treatments are the approaches which do not require to measure all co-ordinates of the structure (Kidder, 1973; Baruch, 1998). This feature is of paramount importance when investigating the location of damage in large, multidimensional structures such as machine tools since, in general, the number of sensors available is a constrained number. Hence, one has to derive information on damage on the basis of incomplete measurements.

The paper presents an application of the Projective Input Residual Method (PIRM) (Oeljeklaus, 1998), which handles the problem of measurement incompleteness, to the fault diagnosis of a machine tool. The application of the projection onto the subspace (Kurnik, 1997) is focused on the reduction of the problem dimensionality to formulate it uniquely. The PIRM can also be effectively used in the procedure of experimental updating of structural parameters that describe the computational model of an object. Then, the parameters charged with errors resulted from inaccurate estimation conducted on the basis of literature data can be treated similarly to "damaged" parameters.

2. Mathematical model

As previously mentioned, the methods of damage detection are based on the examination of the agreement between the information delivered by the mathematical model and that obtained from the measurements of the real object. This problem consists in the detection of those model parameters which undergo changes as the result of the damage. Many real mechanical systems can be represented by a model built by means of the finite element method or rigid finite element method. The sample model of the milling machine FWD-32J developed by making use of the rigid finite element method is shown in Fig. 1. Mathematical model can be presented in the form

$$\mathbf{M}\ddot{\boldsymbol{U}} + \mathbf{H}\dot{\boldsymbol{U}} + \mathbf{K}\boldsymbol{U} = \boldsymbol{P} \tag{2.1}$$

where

$\mathbf{M}, \mathbf{H}, \mathbf{K}$ – inertia, damping and stiffness matrices, respectively

$\boldsymbol{U}, \dot{\boldsymbol{U}}, \ddot{\boldsymbol{U}}$ – vectors of generalized displacements, velocities and accelerations, respectively

$\boldsymbol{P}$ – vector of the generalized force.

Since the determination of all $3n(n+1)/2$ (n — number of degrees of freedom) elements of $\mathbf{M}$, $\mathbf{H}$, $\mathbf{K}$ matrices for a system of n DOF is a time consuming task, the modelling employed the well known topology elaborated by Natke et al. (1995). Application of the topology is especially convenient when used along with the Rigid Finite Element (RFE) method (Kruszewski et al., 1999), which is practiced in modelling of machine tools. This method assumes that the structure consists of discrete spring-less masses (bodies) connected by mass-less spring-damping elements (SDE). Machine tools are intrinsically amenable to lumped parameter representations, comprising rigid massive structural members such as beds, columns etc., connected by light compliant interfaces at guideways, slides etc. The advantage of the RFE is the preservation of the geometrical similarity of the physical model and the real object, which significantly simplifies the localization of the damaged elements of the examined object (Marchelek, 1991).

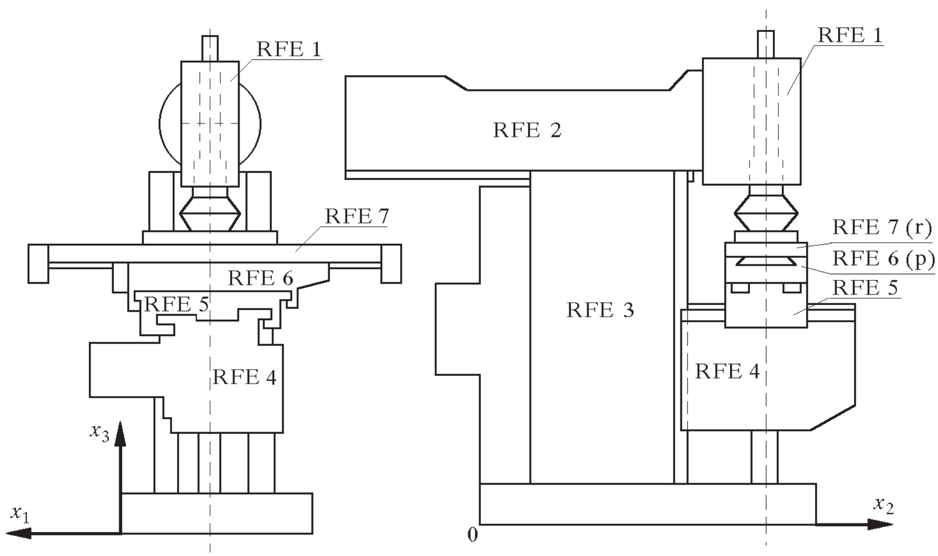

Fig. 1. Model of the FWD-32 J milling machine in the RFE method

The initial computational model described by equation (2.1) is built of a sum of $n \times n$ matrices

$$\mathbf{M} = \sum_{i=1}^{\mu} \mathbf{M}_i^* \qquad \mathbf{H} = \sum_{j=1}^{\beta} \mathbf{H}_j^* \qquad \mathbf{K} = \sum_{k=1}^{\beta} \mathbf{K}_k^* \tag{2.2}$$

where μ is the number of rigid finite elements, β – the number of spring-damping elements

$$\begin{aligned}
\mathbf{M}_i^* &= \mathrm{diag}\,[\mathbf{0},\mathbf{0},...,\mathbf{0},\underbrace{\mathbf{M}_i}_{\text{block No. } i},\mathbf{0},...,\mathbf{0}]\\
\mathbf{M}_i &= \mathrm{diag}\,[m_{1i},m_{2i},m_{3i},m_{4i},m_{5i},m_{6i}]
\end{aligned} \tag{2.3}$$

$$\mathbf{H}_j^* = \begin{array}{cc}
\left[\begin{array}{ccccccccccc}
\mathbf{0} & \cdots & \mathbf{0} & \mathbf{0} & \mathbf{0} & \cdots & \mathbf{0} & \mathbf{0} & \mathbf{0} & \cdots & \mathbf{0}\\
\vdots & \vdots & \vdots & \vdots & \vdots & \vdots & \vdots & \vdots & \vdots & \vdots & \vdots\\
\mathbf{0} & \cdots & \mathbf{0} & \mathbf{H}_{jpp} & \mathbf{0} & \cdots & \mathbf{0} & -\mathbf{H}_{jpr} & \mathbf{0} & \cdots & \mathbf{0}\\
\vdots & \vdots & \vdots & \vdots & \vdots & \vdots & \vdots & \vdots & \vdots & \vdots & \vdots\\
\mathbf{0} & \cdots & \mathbf{0} & \mathbf{H}_{jrp} & \mathbf{0} & \cdots & \mathbf{0} & \mathbf{H}_{jrr} & \mathbf{0} & \cdots & \mathbf{0}\\
\vdots & \vdots & \vdots & \vdots & \vdots & \vdots & \vdots & \vdots & \vdots & \vdots & \vdots\\
\mathbf{0} & \cdots & \mathbf{0} & \mathbf{0} & \mathbf{0} & \cdots & \mathbf{0} & \mathbf{0} & \mathbf{0} & \cdots & \mathbf{0}
\end{array}\right] &
\begin{array}{c}
\\ \\ \text{horizontal band No. } p \\ \\ \text{horizontal band No. } r \\ \\ \\
\end{array}\\
\begin{array}{ccc}
\text{vertical band No. } p & & \text{vertical band No. } r
\end{array} &
\end{array}$$

The matrix $\mathbf{M}_j^*$ is located between the rigid elements p and r. For details concerning the structure of the matrices $\mathbf{H}_{jpp}$, $\mathbf{H}_{jpr}$, $\mathbf{H}_{jrp}$ and $\mathbf{H}_{jrr}$ (see Kruszewski et al., 1986). The matrix $\mathbf{K}_k^*$ has the same form as the matrix $\mathbf{H}_j^*$.

Once the model of the machine tool is constructed, its validity is often checked by comparing its dynamic characteristics with those obtained from an experiment. If the correlation between these two is poor, then the model must be corrected, which is known also as the model updating. The system matrices are corrected in the computational model independently by the dimensionless correction factors

$$\mathbf{M}(a) = \sum_{i=1}^{\mu} a_i \mathbf{M}_i^* \qquad \mathbf{H}(a) = \sum_{j=1}^{\beta} a_j \mathbf{H}_j^* \qquad \mathbf{K}(a) = \sum_{k=1}^{\beta} a_k \mathbf{K}_k^* \tag{2.4}$$

Hence, the dynamic stiffness matrix in the frequency domain has the form

$$\begin{aligned}
\mathbf{S}_\omega(a) &= -\omega^2\mathbf{M}(a) + j\omega\mathbf{H}(a) + \mathbf{K}(a) =\\
&= \sum_{i=1}^{\mu} a_i(-\omega^2\mathbf{M}_i^*) + \sum_{j=1}^{\beta} a_i(j\omega\mathbf{H}_j^*) + \sum_{k=1}^{\beta} a_k\mathbf{K}_k^*
\end{aligned} \tag{2.5}$$

3. Projective input residual method

If all output components are measured, the classical input residual method can be applied as the minimization of the L_2 norm of $\boldsymbol{P}^M - \mathsf{S}_\omega(a)\boldsymbol{U}^M$, where $\boldsymbol{P}^M$ and $\boldsymbol{U}^M$ are the measured vectors of excitation and displacements, respectively.

If not even component of the displacement vector $\boldsymbol{U}^M$ measured, then

$$\mathsf{S}_\omega(a)\boldsymbol{U}^M = \mathsf{S}_\omega(a)\mathsf{C}^\top\mathsf{C}\boldsymbol{U}^M + \mathsf{S}_\omega(a)\overline{\mathsf{C}}^\top\overline{\mathsf{C}}\boldsymbol{U}^M \tag{3.1}$$

where the matrix $\mathsf{C} \in \{0,1\}^{m\times n}$, and m is the number of the measured displacements. The matrix C consists of m rows with 1 corresponding to the measured coordinate, $\overline{\mathsf{C}}$ is the complementary matrix to C. The sample matrix C for a $n = 5$ degree of freedom system and $m = 3$ measured co-ordinates can have the form

$$\mathsf{C} = \begin{bmatrix} 1 & 0 & 0 & 0 & 0 \\ 0 & 1 & 0 & 0 & 0 \\ 0 & 0 & 0 & 0 & 1 \end{bmatrix} \tag{3.2}$$

and its complementary matrix

$$\overline{\mathsf{C}} = \begin{bmatrix} 0 & 0 & 1 & 0 & 0 \\ 0 & 0 & 0 & 1 & 0 \end{bmatrix} \tag{3.3}$$

Hence, the matrix $\mathsf{S}_\omega(a)\mathsf{C}^\top\mathsf{C}\boldsymbol{U}^M$ corresponds to the measured $\mathsf{C}\boldsymbol{U}^M$ displacements, while $\mathsf{S}_\omega(a)\overline{\mathsf{C}}^\top\overline{\mathsf{C}}\boldsymbol{U}^M$ includes the unmeasured $\overline{\mathsf{C}}\boldsymbol{U}^M$ displacements. Thus, it is known that

$$\mathsf{S}_\omega(a)\boldsymbol{U}^M \in \varepsilon_a$$

where ε_a is the set of calculated inputs, determined as

$$\varepsilon_a = \Big\{\mathsf{S}_\omega(a)\mathsf{C}^\top\mathsf{C}\boldsymbol{U}^M + \boldsymbol{P}_0 \ : \quad \boldsymbol{P}_0 \in R\Big(\mathsf{S}_\omega(a)\overline{\mathsf{C}}^\top\Big)\Big\} \tag{3.4}$$

where $R\Big(\mathsf{S}_\omega(a)\overline{\mathsf{C}}^\top\Big)$ is the image of $\mathsf{S}_\omega(a)\overline{\mathsf{C}}^\top$. The aim functional of the projective input residual method is defined as follows

$$J_c(a) = \min_{P^\gamma\in\varepsilon_a} \|\boldsymbol{P}^M - \boldsymbol{P}^\gamma\|_2^2 = \mathrm{dist}(\boldsymbol{P}^M, \varepsilon_a)^2 \tag{3.5}$$

where $\boldsymbol{P}^\gamma$ is the calculated input vector (force) that is equal to the distance between $\boldsymbol{P}^M$ and the vector space $\varepsilon_a \cdot [\mathsf{C}\mathsf{F}_\omega(a)]^{-1}$ (see Fig. 2), where $\mathsf{F}_\omega(a) =$

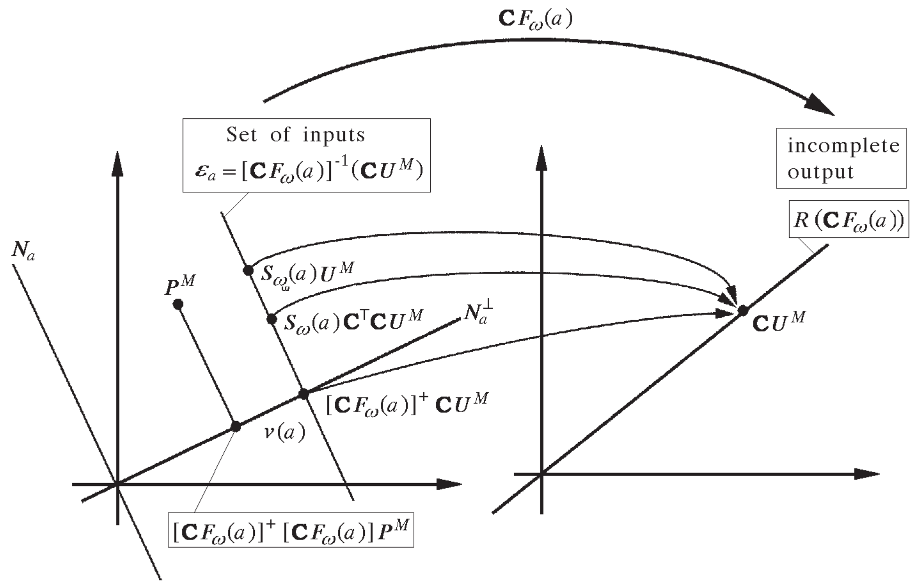

Fig. 2. Illustration of the projective input residual method (Oeljeklaus, 1998)

$\mathbf{S}_\omega^{-1}(a)$, is not the inverse of $[\mathbf{CF}_\omega(a)]$, which does not exists, but it is a map of the $R([\mathbf{CF}_\omega(a)])$ (an image of the $[\mathbf{CF}_\omega(a)]$) onto the domain of $[\mathbf{CF}_\omega(a)]$.

$J_c(a)$ can be calculated as

$$J_c(a) = \Big\| \boldsymbol{P}(a)(\boldsymbol{P}^M - \mathbf{S}_\omega(a)\mathbf{C}^\top\mathbf{C}\boldsymbol{U}^M) \Big\|_2^2 \tag{3.6}$$

where $\boldsymbol{P}(a)$ is the projector onto $N_a^\perp$ (see Fig. 2), which is the orthogonal complement of $N_a = R(\mathbf{S}_\omega(a)\overline{\mathbf{C}}^\top)$ – kernel of $\mathbf{CF}_\omega(a)$.

Thus

$$\boldsymbol{P}(a) = [\mathbf{CF}_\omega(a)]^+[\mathbf{CF}_\omega(a)] \tag{3.7}$$

where $[\mathbf{CF}_\omega(a)]^+$ is the Moore-Penrose pseudo-inverse matrix.

Therefore, we obtain

$$J_c(a) = \Big\| [\mathbf{CF}_\omega(a)]^+[\mathbf{CF}_\omega(a)]\boldsymbol{P}^M - [\mathbf{CF}_\omega(a)]^+\mathbf{CU}^M) \Big\|_2^2 \tag{3.8}$$

The residuum $\boldsymbol{v}(a) = \boldsymbol{P}(a)(\boldsymbol{P}^M - \mathbf{S}_\omega(a)\mathbf{C}^\top\mathbf{C}\boldsymbol{U}^M)$ is a non-linear function due to the non-linearity of $P(a)$. Thus, the minimization of $J_c(a)$ consists in the following non-linear optimization find

$$\widehat{a} = \arg\min_a v^H(a)v(a) \tag{3.9}$$

Moreover, the partial derivatives are determined

$$v^{\upsilon} = \frac{\partial v(a)}{\partial a_{\upsilon}} \qquad \upsilon = 1, ..., n_p \tag{3.10}$$

which are especially important when using the methods such as sequential linear programming or the Levenberg-Marquardt method.

4. Damage indicator

The aim of the damage indication is not an accurate system identification but the damage location that is equivalent to the determination of parameters that have changed with respect to the original model. Since the gradients $v^{\nu}(a)$ are very sensitive to the structural changes, therefore they can be used for the damage detection and can be applied in the form of the indicator

$$\tau_{\nu} = \frac{\|v^{\nu}(\mathbf{1})\|}{\|v_D^{\nu}(\mathbf{1})\|} \geqslant 0 \tag{4.1}$$

where $v_D(a)$ are the residuals of the measured $\boldsymbol{U}_D^M$ of the probably damaged structure for the excitation vector $\boldsymbol{P}^M$, which was also used to excite the undamaged structure $(\boldsymbol{U}^M)$.

Since $\|v_D^{\nu}(\mathbf{1})\|$ is always different from 0, the proposed indicator is determined uniquely. Because of measurement errors, $\|v^{\nu}(\mathbf{1})\|$ is a real number greater than zero, and its division by $\|v_D^{\nu}(\mathbf{1})\|$ which is calculated for the $\boldsymbol{U}_D^M$ corresponding to the damaged system, gives information on which parameter is changed and, in consequence, localizes the damage. If the damage does not exist, one can expect that $\|v^{\nu}(\mathbf{1})\| \approx \|v_D^{\nu}(\mathbf{1})\|$ and $\tau \approx 1$. Otherwise $0 < \tau_{\nu} \ll 1$, since $\|v^{\nu}(\mathbf{1})\| \ll \|v_D^{\nu}(\mathbf{1})\|$.

5. Measurement data preparation and damage simulation

The milling machine was excited using an electrohydraulic exciter located between bodies No. 1 and 7, which were the head and the table of the machine, respectively. The hydraulic exciter produced a force impulse (very short time of action) of 370 daN amplitude. Its location is given in Fig. 3. The exciter was located along the direction corresponding to the direction of the resultant

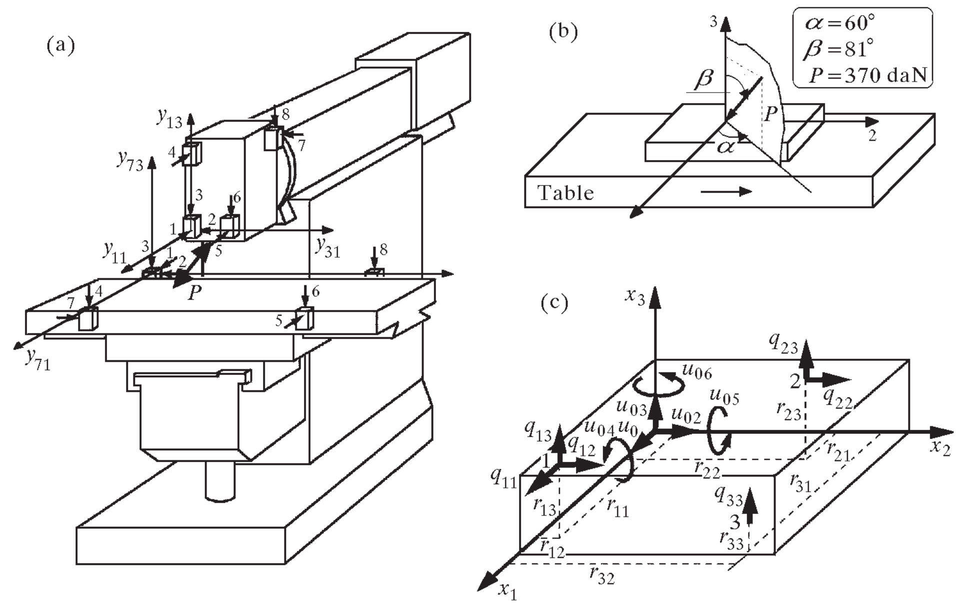

Fig. 3. Scheme of the experimental stand (a) location of the sensors and excitation force $\boldsymbol{P}$, (b) direction of the excitation force $\boldsymbol{P}$, (c) transformation of the measured displacements $\boldsymbol{q}$ to the displacement vector $\boldsymbol{u}$

cutting force (Fig. 3b). This made that the results of the analysis reflect real machining conditions. The displacements of bodies No. 1 and 7 were measured. For this purpose 16 sensors were used (8 for each body). This enabled more accurate determination of the displacements of the measured bodies. The minimum number of sensors required was 6 (Fig. 3c). The relative locations of the sensors that measure the displacements of the head are shown in Figure 3a. After FFT (frequency range 1-300 Hz) of the displacements of the head and the table and their transformations into the generalized co-ordinate system the results were recorded. Hence, 6 complex characteristics for the head and the table in the frequency range 1-300 Hz were registered (see Fig. 4). It means that 12 of 42 co-ordinates were measured. The detailed description of the experimental investigations and signal processing can be found in (Gutowski and Berczyński, 1995).

The force impulse can be approximated with the Dirac function because of a very short time of duration. The Fourier transform of such a signal is 1. That unit force (in the frequency domain) acted simultaneously on the head and table but in the opposite directions. Since the model was built in the generalized co-ordinate system there was a necessity (as for displacements) to

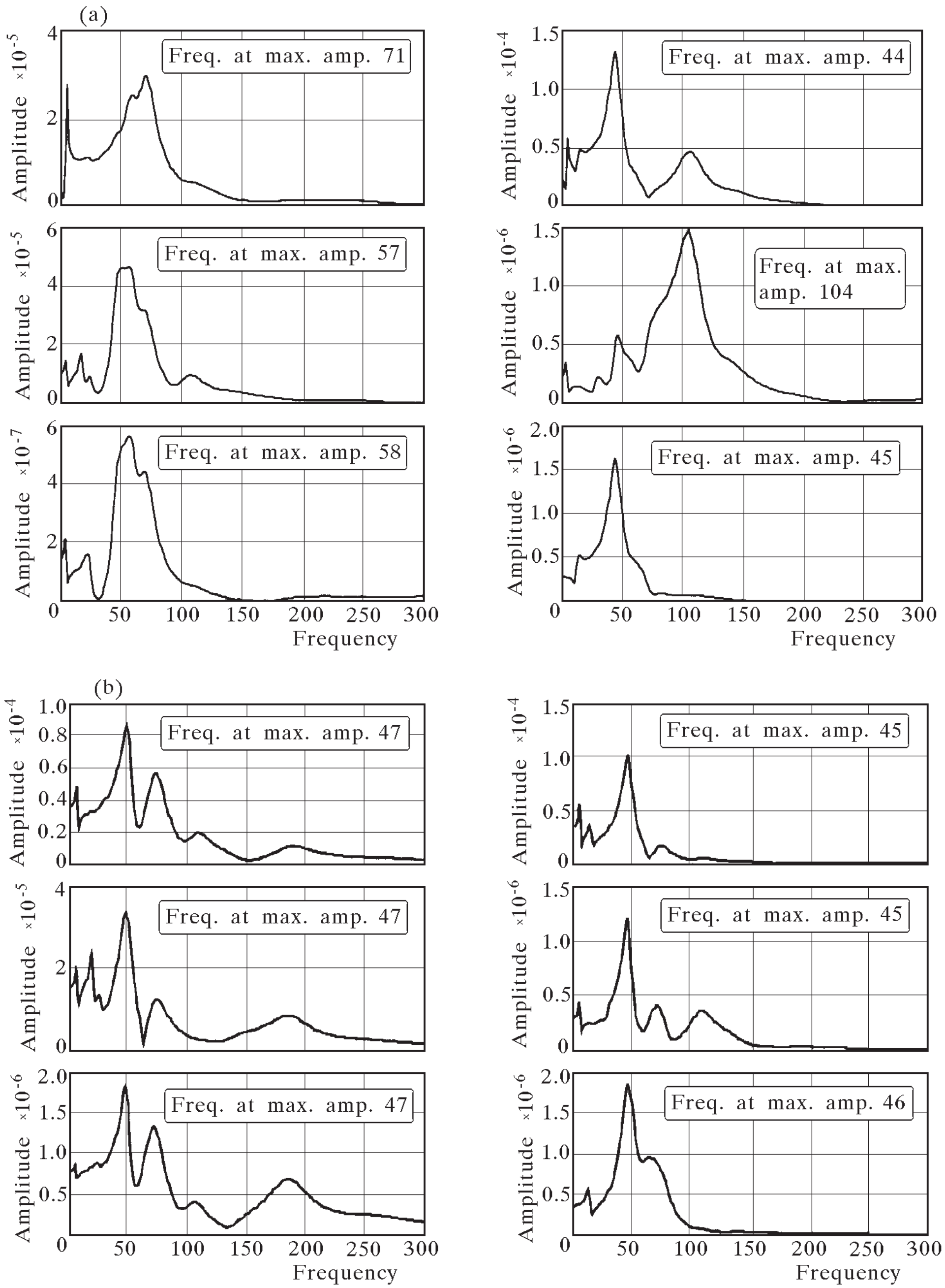

Fig. 4. AF characteristics of (a) head (b) table of the milling machine

transform the excitation vector to the gravity centers of the excited bodies. The transform resulted in the excitation vector $(n \times 1)$ that contained 12 non-zero elements: 1-6 excitation components of the head (body No. 1) and 37-42 excitation components of the table (body No. 7).

To minimize the errors of measurements the displacements for $N = 4$ resonance frequencies were assumed for further analysis. It was so, because the coherence function for those resonance frequencies was close to 1, which meant that the influence of noise and other error carrying factors was small. It resulted in N complex displacement vectors with 12 non-zero elements. Since there were no measurements taken from the damaged machine tool there was a need to simulate them. The simulation considered the changes appearing during the exploitation of the machine.

The relative locations of the elements that constitute a slideway connection are associated with friction forces. Therefore the machine tool is accompanied with progressing wear of co-operating elements. Thus, a lower stiffness of the contact joint is reflected in the measurements by higher values of the displacements of the adjacent bodies.

The displacements of the worn elements were simulated by multiplying the displacements that were measured for the elements of the unworn machine. To simulate the wear of the slideway connection between bodies No. 6 and 7, elements No. 37-42 (table) of the displacement vector were multiplied by 2, which was the representative for damage at that location of the milling machine. The wear of the head was simulated similarly, and components No. 1-6 were subjected to the amplification. In both simulations the modified displacement vector was denoted $\boldsymbol{U}_D^M$.

6. Examination results

It appears that some groups of parameters are responsible for the larger values of the table displacements (Fig. 5a) and their changes, in comparison with the undamaged machine, which was detected by the proposed indicator. The first group consists of stiffness elements No. 8, 9, 10, 11 and the corresponding damping parameters 38, 39, 40, 41 that describe the contact properties of bodies No. 6 and 7 (slideway connection). It could be expected as their lower values resulted in higher values of the table displacements. Higher values of the displacements of the table can also be caused by the damage in the connection of bodies No. 5 and 6. The parameters characterising this connection (No. 12 – stiffness and No. 42 damping) are strongly coupled with the parameters from

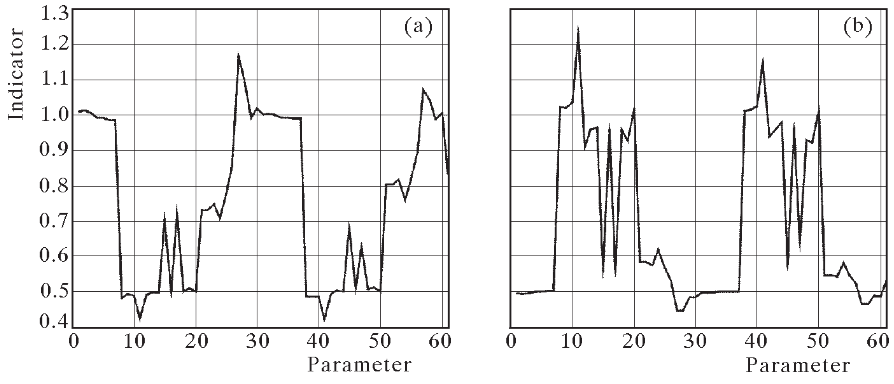

Fig. 5. Values of the damage indicator for (a) table; (b) head of the milling machine

the first mentioned group by the displacements of body No. 6 (base of the slideway connection 6-7). The indicator also detected the damage to slideway connection of bodies 4 and 5 (stiffness parameters No. 12, 13, 14, 16, 18, 19, 20 and corresponding damping parameters No. 42, 43, 44, 46, 48, 49, 50). This can be explained by the high value of the stiffness of the bolted connection between bodies 5 and 6 (about 100 times greater than the stiffness of the connection of body 4 and 5). It causes that bodies 5 and 6 behave almost like one rigid element, which automatically couples the parameters of the slideway connection of bodies 4 and 5 with the displacements of the table.

The indicator detected damage (for the increased displacements of the head) in the following elements (Fig. 5b): 1-8, 21-38, 51-60. Stiffness parameter 1 and damping parameter 31 characterise the physical properties of the connection of the head (body No. 1) with the horizontal beam (body No. 2). These parameters influence directly the displacements of the head. Motion of the head depends also on the stiffness parameters (parameters No. 2-8) and the corresponding damping parameters (parameters No. 32-38). It is obvious that higher values of the amplitudes of the head along the x_1 axis might be caused by the lower stiffness of the slideway connection between body 3 and 4.

References

1. Baruch M., 1998, Damage detection based on reduced measurements, *Mechanical Systems and Signal Processing*, **12**, 23-46

2. Doebling S.W, Farrar C.R., Prime M.B., Shevitz D.W., 1996, Damage identification and health monitoring of structural and mechanical systems from changes in their vibration characteristics: a Literature Review, Report No. LA-13070- MS, Los Alamos National Laboratory
3. Gutowski P., Berczyński S., 1995, Parameters identification of dynamic models of machine tool supporting systems, *Proceedings of the Ninth World Congress on the Theory of Machines and Mechanisms*, Politecnico di Milano, Italy, 2, 1349-1354
4. Kidder R.L., 1973, Reduction of structural frequency equations, *American Institute of Aeronautics and Astronautics*, **32**, 892
5. Kruszewski J.I. et al., 1999, *Rigid Finite Element Method in Dynamics of Construction*, (in Polish) Warsaw, WNT
6. Kurnik W., 1997, *Divergent and Oscillational Biffurcation*, (in Polish) Warsaw, WNT
7. Li C., Smith C., Smith S.W., 1995, Hybrid approach for damaged detection in flexible structures, *Journal of Guidance, Control and Dynamics*, **18**, 419-425
8. Marchelek K., 1991, *Machine Tool Dynamics*, (in Polish) Edition 2. Warsaw, WNT
9. Natke H.G., Collman D., Zimmerman H., 1995, Beitrag zur korrektur des rechenmodells eines elastomechanischen systems anhand von versuchsergebnissen, *VDI-Berichte*, **221**, 23-32
10. Natke H.G., Tomlinson G.R., Yao J.T.P., 1993, *Safety Evaluation Based on Identification Approaches Related to Time-Variant and Nonlinear Structures*, Wiesbaden, Vieweg
11. Oeljeklaus M., 1998, Ein Beitrag zur Systemidentifikation: Das Projektive Einganggrossenverfahren und das Regularisierte Ausganggrossenverfahren im Frequenzbereich fur unvollstandige Messungen. Habilitation, Universitat Hannover,. Reports of the Curt-Risch-Institute of the University of Hannover: CRI-F- 3/99

Zastosowania rzutowanego residuum sygnału wejściowego do diagnostyki uszkodzeń układów mechanicznych

Streszczenie

W pracy przedstawiono zastosowanie metody rzutowanego residuum sygnału wejściowego do wykrywania uszkodzeń na podstawie niekompletnych pomiarów obiektu (liczba pomierzonych sygnałów jest mniejsza niż liczba stopni swobody modelu badanego układu mechanicznego) oraz do wskazania parametrów opisujących model

obliczeniowy, wymagających modyfikacji przy praktycznej realizacji procedur identyfikacji parametrycznej. Metoda nie wymaga redukcji liczby stopni swobody modelu matematycznego, a tym samym identyfikowane parametry zachowują interpretację fizyczną. Zaproponowany wskaźnik służący do lokalizacji uszkodzonego elementu porównuje pochodne cząstkowe residuów wielkości wejściowych dla modelu bez uszkodzeń z modelem reprezentującym obiekt z uszkodzeniami. Rozważania teoretyczne zilustrowane są przykładem obliczeniowym dla frezarki FWD-32J.

Manuscript received May 15, 2000; accepted for print August 14, 2001